BIOACTIVE COATING WITH ANTIMICROBIAL EFFECT FOR STAINLESS STEEL: PREPARATION AND CHARACTERIZATION

Maxim V. MAXIMOV[1,2], Oana-Cristina MAXIMOV[2], Roxana Doina TRUȘCĂ[1,3], Denisa FICAI[1,3], Anton FICAI[1,3,*]

This study focuses on the development of bioactive coatings with antimicrobial properties on stainless steel substrates. Initially, 45S5 bioactive glass was applied to stainless steel discs via spin coating, followed by thermal treatment to stabilize the coating. Subsequently, a layer of Miramistin, an antimicrobial agent, was added. The coatings were characterized using scanning electron microscopy (SEM) and Fourier-transform infrared microscopy. In vitro tests confirmed the bioactive properties of the coatings. The proposed method resulted in uniform coatings without macrocracks, exhibiting both antimicrobial and bioactive properties.

Keywords: bioactive glass coatings, stainless steel, Miramistin, antibacterial, FT-IR microscopy

1. Introduction

Any surgical intervention carries a significant risk of bacterial contamination, which can lead to infections, inflammation, and a prolonged healing period. In this context, the antimicrobial properties of implantable materials represent a considerable advantage. Bioactive glass 45S5, known for its ability to promote integration into biological tissues, also possesses antimicrobial properties [1-5]. To enhance these characteristics, glass doping techniques can be employed or an additional antimicrobial drug can be applied to the implant surface [6-8]. Miramistin (Fig. 1) is a topical antiseptic with a broad spectrum of antimicrobial activity, including efficacy against biofilms and good local tolerability. It was originally developed during the Soviet Union's Cold War space program and, although it is used clinically in various countries of the former Soviet bloc, remains relatively unknown in other countries [9-12]. This approach of combining bioactive glass with Miramistin has the potential to improve the antimicrobial performance of the material, providing additional protection in surgical applications.

The toxicity of Miramistin is relatively low, for example LD50 of 1200 mg/kg for rats, 1000 mg/kg for mice and 100 g/L for fish [9]. In this context, we consider that Miramistin could be used as an adjuvant substance to improve the

* Correspondence: anton.ficai@upb.ro
[1] Department of Science and Engineering of Oxide Materials and Nanomaterials, National University of Science and Technology POLITEHNICA Bucharest, Romania;
[2] SC Microsin SRL, Bucharest, Romania
[3] Academy of Romanian Scientists, Bucharest, Romania

antimicrobial action of bioactive glass coatings. To date, Miramistin has not been used in the manufacture of implants, although it has multiple clinical applications due to its antimicrobial, antiseptic and disinfectant properties.

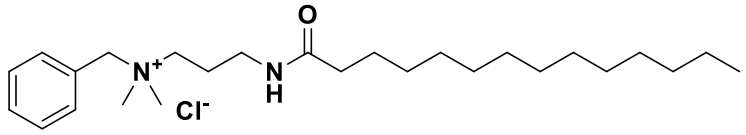

Fig. 1. Chemical structure of Miramistin

In this study, we propose a dual-layer coating system composed of 45S5 bioactive glass and Miramistin, applied on stainless steel supports. The aim is to assess the morphology, composition, and bioactivity of the coatings, highlighting the potential of Miramistin to enhance the antimicrobial performance of bioactive surfaces.

2. Materials and Methods

The following reagents were used in the experiments: tetraethyl orthosilicate (TEOS; 99.9%) from VWR (Radnor, PA, USA), triethyl phosphate (TEP; 99%), nitric acid (65%), tris(hydroxymethyl) aminomethane (TRIS; 99%), acetone (99.8%), hydrochloric acid (37%), all from Merck (Darmstadt, Germany); calcium nitrate tetrahydrate (99%), sodium chloride (99%), calcium chloride dihydrate (99%) all from Sigma-Aldrich (St. Louis, MO, USA); sodium nitrate (99.5%), potassium chloride (99%), sodium bicarbonate (99%), potassium phosphate dibasic (99%), sodium sulfate (99%), all from SILAL (Bucharest, Romania); magnesium chloride hexahydrate (99%) from Fluka (Charlotte, NC, USA); and Miramistin (99.9%) from SC Microsin SRL.

2.1. Bioactive Glass Preparation

15.6g (0.075mol) tetraethylorthosilicate was gradually added to a mixture of 30.0 g (1.67 mol) demineralized water and 0.2 mL of 2N nitric acid heated to 40°C, over a period of 1.5-2 hours. After the addition was complete, the solution was stirred for 30 minutes. Subsequently, 1.54g (0.0085mol) triethyl phosphate was added over a period of 10–15 minutes. The reaction mixture was stirred for another 60 minutes at 40°C. To the resulting solution, 10.32 g (0.044 mol) of calcium nitrate tetrahydrate was gradually added, with each portion being added after the previous one had completely dissolved. After 15 minutes, 6.72g (0.079mol) of sodium nitrate were added in a similar manner. The reaction mass was stirred for another 30 minutes at 40°C, then cooled to 25–30°C and stirred for 24 hours. The resulting solution was deposited on stainless steel support.

2.2. Stainless Steel Supports Preparation

For the experiments, AISI 304L stainless steel discs, measuring 25 mm × 1.5 mm, were used as supports for bioactive glass coating. The surfaces of the discs were polished with 320-grit abrasive paper, then degreased in an aqueous detergent solution, followed by immersion in 0.5 M hydrochloric acid solution for surface activation [13]. After activation, the discs were rinsed with demineralized water, ultrasonicated in acetone for 20 minutes and finally dried. The samples prepared in this way were used for coating application.

2.3. Coating stainless steel supports with bioactive glass

The solution prepared according to the procedure detailed in subchapter 2.1 was used to coat the stainless steel supports using the spin-coating technique. The bioactive glass coatings were applied using a spin-coater model SPIN150i, from the company POLOS.

Before coating, the stainless steel supports, prepared according to the procedure detailed in subchapter 2.2, were mounted on the rotating plate of the spin-coater and fixed by suction using a vacuum pump. 0.5–1 mL of bioactive glass solution was applied to the surface of the supports at an initial speed of 100 rpm. The rotation speed was then gradually increased by 200 rpm until it reached 2500 rpm during the EBR (edge bed removal) and drying stage. The samples were rotated at this speed for 45 seconds to remove excess solution from the sample surface and evaporate the solvent. In total, two layers were applied, and the samples were dried at 130°C for 22 hours.

To stabilize the bioactive glass coatings, the samples were subjected to a heat treatment at 700°C for 3 hours, with a heating rate of 5°C/minute. After cooling, the resulting surfaces were analyzed by scanning electron microscopy (SEM) and FTIR microscopy.

2.4. Miramistin Deposition on Bioactive glass – coated supports

The deposition of antiseptic (Miramistin) on bioglass-coated supports was carried out by immersion in an acetone solution of antiseptic. The solution was prepared by dissolving 1 g of Miramistin in 25 mL of acetone. To allow adequate absorption of the substance over the entire surface, the samples were immersed for approximately 10 minutes in the solution preheated to 30–35°C. After deposition, the samples were extracted at a uniform speed of 10 cm/minute. Subsequently, the samples were dried at room temperature. To assess the uniformity and quality of the applied Miramistin layer, the obtained coatings were analyzed by FTIR and SEM microscopy.

2.5. Bioactivity Evaluation and Surface Characterization

To evaluate the bioactivity of the samples obtained, in vitro tests were performed by immersing the samples in simulated body fluid (SBF) solution for periods of time ranging from 1 and 14 days, at 36±1°C. Each sample was placed in a polypropylene container with a lid, containing 20 mL of SBF solution. During the tests, the pH and conductivity of the SBF solution in which the samples were immersed were monitored. After the test was completed, the surface of the samples was analyzed by FTIR and SEM microscopy.

The surfaces obtained in this study were analyzed by FT-IR microscopy using a Nicolet iN10MX device, manufactured by Thermo Scientific. The detector used was cooled with liquid nitrogen, the data collection mode was reflectance. For each sample, a randomly selected area measuring 150 µm × 150 µm was analyzed.

The morphology of the obtained surface was analyzed using a QUANTA INSPECT F50 scanning electron microscope, equipped with a field emission gun, with a resolution of 1.2 nm and an energy dispersive X-ray spectrometer with a MnK resolution of 133 eV.

3. Results and discussion

3.1.Determination of pH Variation and Ionic Conductivity

To evaluate the bioactivity of the obtained coatings, the samples were immersed in SBF solution for periods of 1, 2, 3, 7 and 14 days. The SBF solution was prepared according to the protocol described in the literature, and the temperature during the experiment was maintained constant at 36±1°C [14]. During the analysis, variations in the pH and conductivity of the immersion solution were monitored. The evolution of pH as a function of exposure time is shown in Fig. 2a.

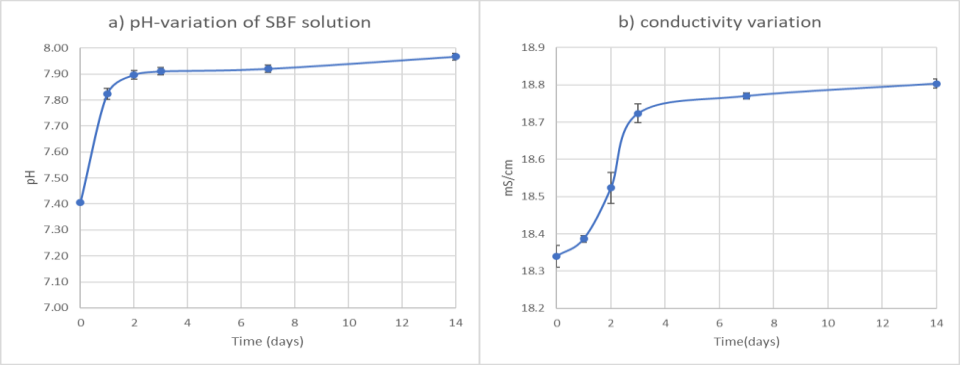

Fig. 2. a) pH variation of SBF solution after immersion of samples coated with bioactive glass and Miramistin for different time intervals; b)conductivity variation of the SBF solution during the bioactivity evaluation of samples coated with bioactive glass and Miramistin.

The graphical representation in Fig. 2a highlights a slight increase in pH from 7.4 to 7.9 in the first two days after immersion, followed by an even slower increase, reaching a value of 8.0 after 14 days. This phenomenon can be attributed to the

release of ions from the bioactive glass composition, which triggers the process of hydroxyapatite formation, thus indicating the manifestation of the bioactive properties of the obtained coating [15].

Analyzing the graphical representation in Fig. 2b, a slight increase in the conductivity of the SBF solution in the first three days, from 18.35 to 18.7 mS/cm, is highlighted, followed by an insignificant variation up to 18.8 mS/cm in the following days, similar to the pH variation. This behavior indicates a rapid release of ions from the bioactive glass, with the manifestation of bioactivity taking place in the first days after the immersion of the samples in SBF. This observation is also confirmed by FTIR and SEM microscopy analyses, which will be discussed further.

3.2. FT-IR Microscopic Evaluation of the Surfaces

After depositing the 45S5 bioactive glass on the stainless steel supports, the obtained coating was characterized using FT-IR microscopy, and the analysis results are presented in Fig. 3.

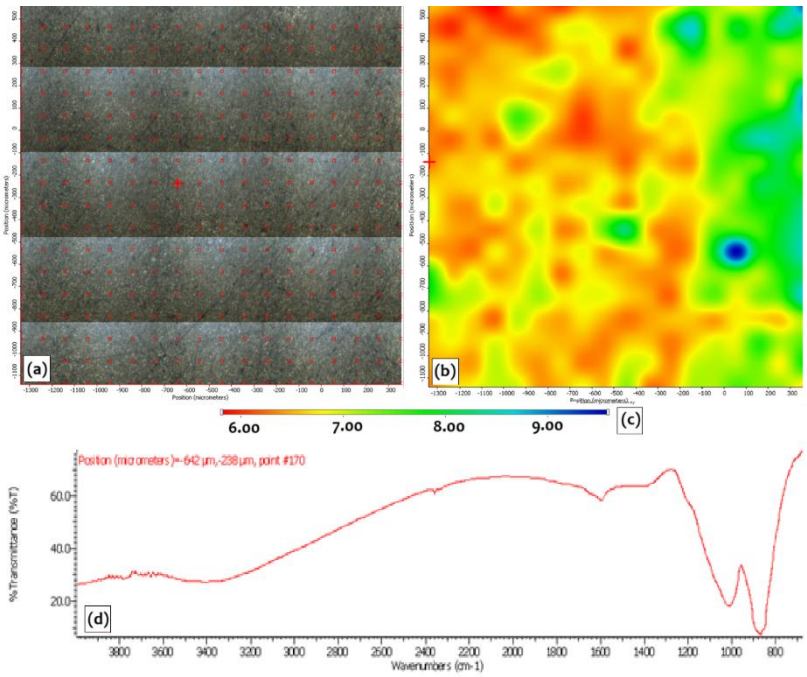

Fig. 3. FTIR microscopy analysis of a randomly selected area of 45S5 bioactive glass coating on stainless steel supports a) video map b) FTIR map at 870cm^{-1} c) FTIR map scale d) FTIR spectra

In Fig. 3a, the video image of the analyzed surface is shown. Fig. 3b shows the FTIR transmittance map, where the color differences correspond to variations in transmittance measured at 870 cm^{-1}. Areas marked in red indicate lower transmittance values, suggesting a higher amount of deposited material, while blue areas correspond to higher transmittance values, indicating regions with thinner or

less dense deposits. The FTIR spectrum of the analyzed surface is shown in Fig. 3d, where the peaks specific to bioactive glass can be observed. The peaks at 870 cm^{-1} and 1070 cm^{-1} correspond to the symmetric and asymmetric stretching vibrations of the Si-O-Si group, respectively. The signals recorded at 1630 cm^{-1} and 3450 cm^{-1} are associated with the presence of O-H bonds, indicating the presence of water in the bioglass composition or hydroxyl groups. Additionally, the narrow band located at 1400 cm^{-1} is characteristic of the carbonate group. The transmittance differences observed on the FTIR map are around 4%, suggesting a relatively uniform thickness of the deposited layer across the analyzed surface. (Fig. 3c).

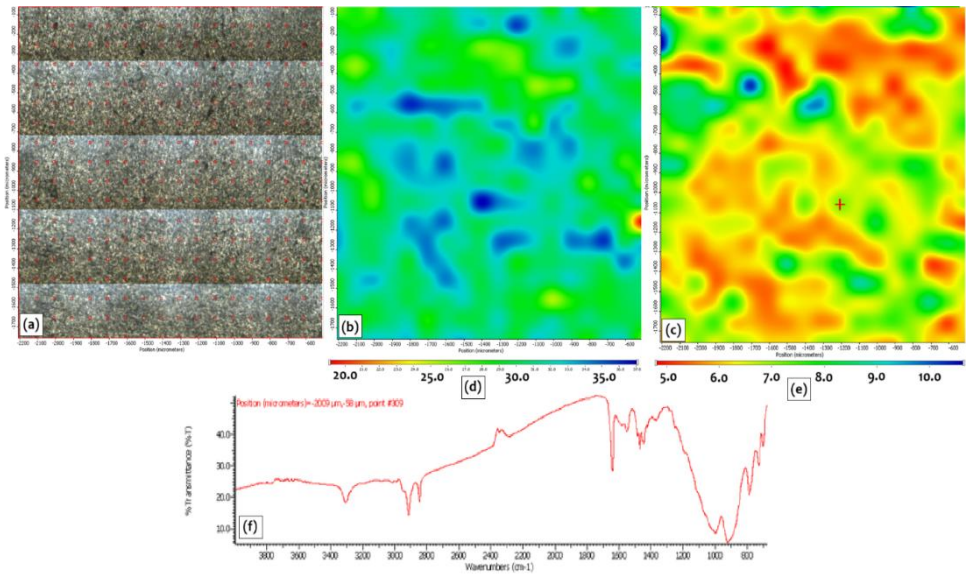

Fig. 4. FTIR microscopy analysis of a randomly selected area on the surface coated with bioactive glass and subsequently treated with Miramistin a) video map b) FTIR map at 1645cm^{-1} c) FTIR map at 906 cm^{-1} d) FTIR map at 1645cm^{-1} scale e) FTIR map at 910cm^{-1} f) FTIR spectra

As previously mentioned, an antimicrobial layer of Miramistin was deposited on the surface of the samples coated with bioactive glass. The obtained coating was investigated by FT-IR microscopy, and the results of the analysis are presented in Fig. 4. The FTIR maps illustrated in Fig. 4b and 4c correspond to peaks located at 1645 cm^{-1} and 910 cm^{-1}, respectively. The first peak is specific to Miramistin, while the second is characteristic of bioactive glass. This was done in order to compare the distribution of the two materials on the surface of the samples.

Analysis of the FTIR maps indicates that Miramistin is relatively uniformly distributed over the entire analyzed surface, with an average transmittance variation of approximately 10% (Fig. 4d). A similar behavior is observed for the bioactive glass, which shows a transmittance variation of around 5% (Fig. 4e).

The obtained FT-IR spectrum highlights the peaks specific to bioactive glass, located at 910 cm^{-1} and 1000 cm^{-1}. A slight shift of these peaks is observed

compared to the initial spectrum (Fig. 3d), which may indicate possible interactions between the coating components. Additionally, the peaks characteristic of Miramistin are present in the IR spectrum. The peaks located at 3305 cm^{-1} and 1600 cm^{-1} correspond to the -NH group, while those at 2915 cm^{-1} and 2850 cm^{-1} are attributed to the asymmetric and symmetric stretching vibrations of the aliphatic C-H group. The sharp peak at 1645 cm^{-1} is specific to the C=O group, and the one at 1550 cm^{-1} indicates the presence of a C=C bond. The asymmetric deformation of the -CH_2 group is highlighted by the peak at 1470 cm^{-1}, and the deformation of the CH_3 group is marked by a low-intensity peak at 1380 cm^{-1} [16, 17]. Thus, the results confirm that the Miramistin layer is distributed over the entire analyzed surface, with minor variations in thickness.

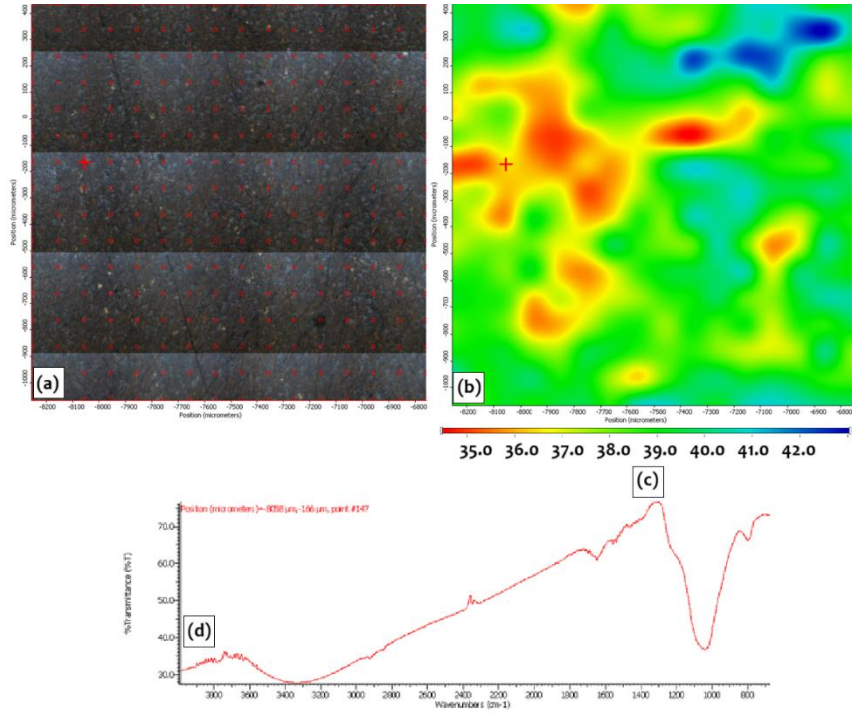

Fig. 5. FTIR microscopy analysis of the surface of samples after immersion in SBF solution a) video map b) FTIR map at 1038cm^{-1} c) FTIR map scale d) FTIR spectra

After the deposition of Miramistin, the samples were subjected to an in vitro bioactivity test by immersion in SBF solution for a period of 14 days. Subsequently, their surfaces were reanalyzed by FT-IR microscopy to verify the formation of a hydroxyapatite layer, which is an indicator of the bioactivity of the obtained coatings. A random area on the surface of each sample was analyzed, and the results obtained are presented in *Fig. 5*. The transmittance variation associated with the formed hydroxyapatite layer ranges between 7–8%, which may indicate slight differences in layer thickness. The FTIR spectrum displays a uniform profile across

the entire analyzed surface. Analyzing the spectrum, the disappearance of the peaks characteristic of Miramistin is observed, which suggests a gradual release of the substance in the SBF environment. The intensity of the peaks specific to bioactive glass (1070 cm^{-1} and 870 cm^{-1}) decreases, being replaced by a single peak that appeared at 1040 cm^{-1}, attributed to the presence of the P-O group. In addition, the IR spectrum highlights the presence of peaks at 3320 cm^{-1} and 1650 cm^{-1}, which are associated with O-H bonds. The intensity of the peak characteristic of the C-O bond, located at 1470 cm^{-1}, is significantly reduced. These observations indicates that, on the surface of the samples, both the desorption of Miramistin and the formation of a new hydroxyapatite layer occurred, thus confirming the bioactivity of the obtained coating.

3.3. Scanning electron microscopy of Surface Morphology

The surface morphology of the samples, after deposition of bioactive glass, Miramistin and immersion in SBF was analyzed by scanning electron microscopy (SEM). Fig. 6a and 6b present SEM images of the bioactive glass layer surface. Fig. 6a, at a magnification of 100x, provides a general perspective on the distribution of the bioactive glass on the surface of the supports. The layer is relatively uniform, without major discontinuities, with only small areas of material accumulation visible. The obtained coating does not exhibit macrocracks. In Fig. 6b, the presence of pores and the rough structure characteristic of bioactive glass can be observed. The adhesion of the layer to the support is good, with no signs of delamination. Fig. 6c and 6d show SEM images of the support surfaces after coating with bioactive glass and Miramistin. Fig. 6c, at a magnification of 100x, provides an insight into the general distribution of Miramistin on the bioactive glass surface. The applied layer is relatively evenly distributed, consistent with the FT-IR microscopy results, which indicate the disappearance of pores in the bioactive glass, most likely as a result of their filling with Miramistin. No significant accumulations or agglomerations are visible. The detailed structure of the Miramistin layer can be seen in Fig. 6d, at a magnification of 10,000x. Small cubic crystals are present on the surface, the composition of which will be discussed in the following sections. Regarding the homogeneity of the layer, the application of Miramistin proved to be effective, with no cracks or visible gaps observed.

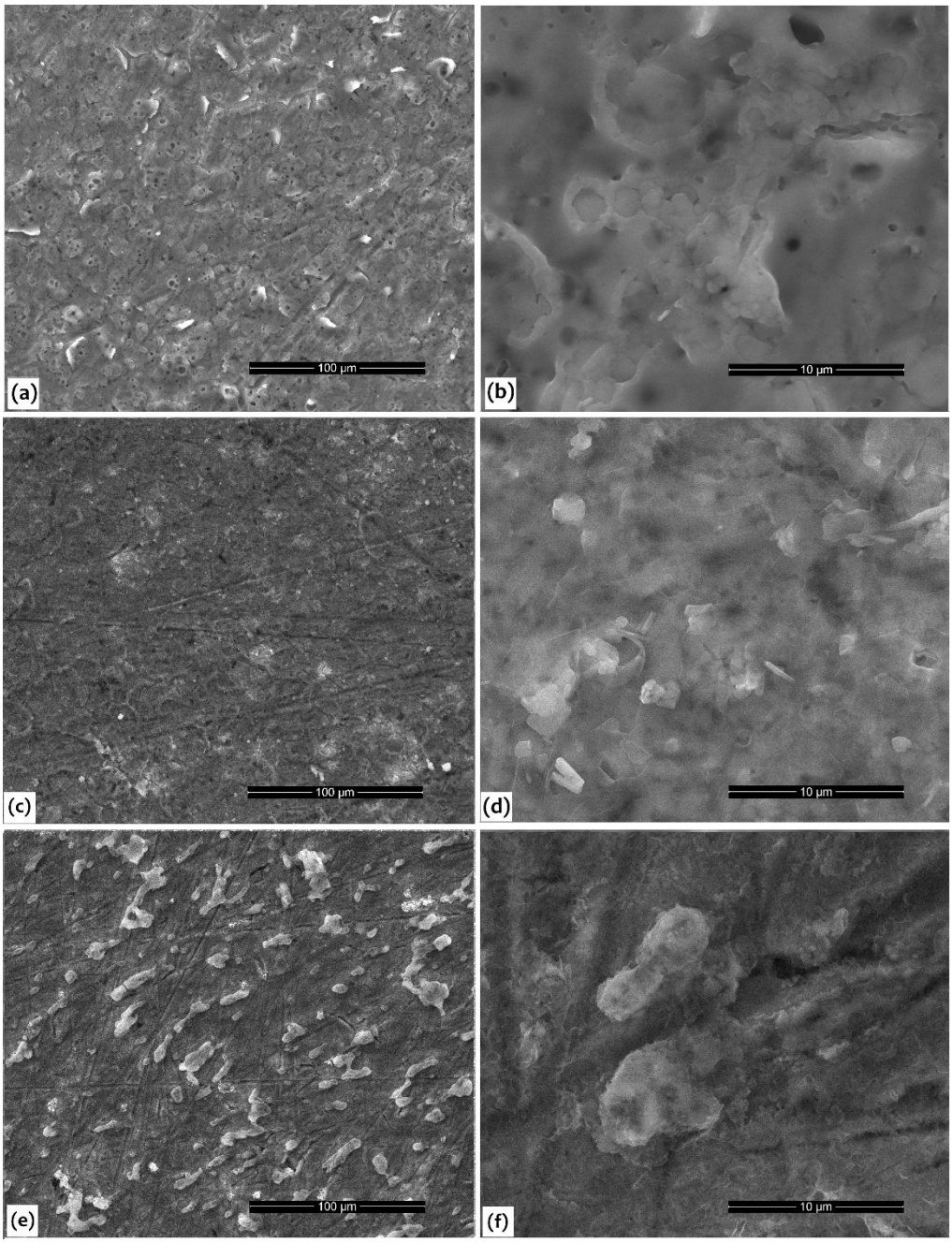

Fig. 6. SEM images of the coating surface: (a, b) bioactive glass; (c, d) after Miramistin coating; (e, f) after 14 days of immersion in SBF.

The surface morphology of the samples after immersion in SBF for 14 days is shown in Fig. 6e and 6f. At a magnification of 100x, small irregularly shaped

agglomerations, ranging in size from 5 to 20 µm, are observed, which may represent hydroxyapatite crystallization centers. The presence of these agglomerations can be attributed to the high surface porosity and, consequently, the high density of nucleation centers, which favor hydroxyapatite formation.

At a magnification of 10,000x (Fig. 6f), a uniform hydroxyapatite coverage is observed across the entire analyzed surface, along with these crystallization centers.

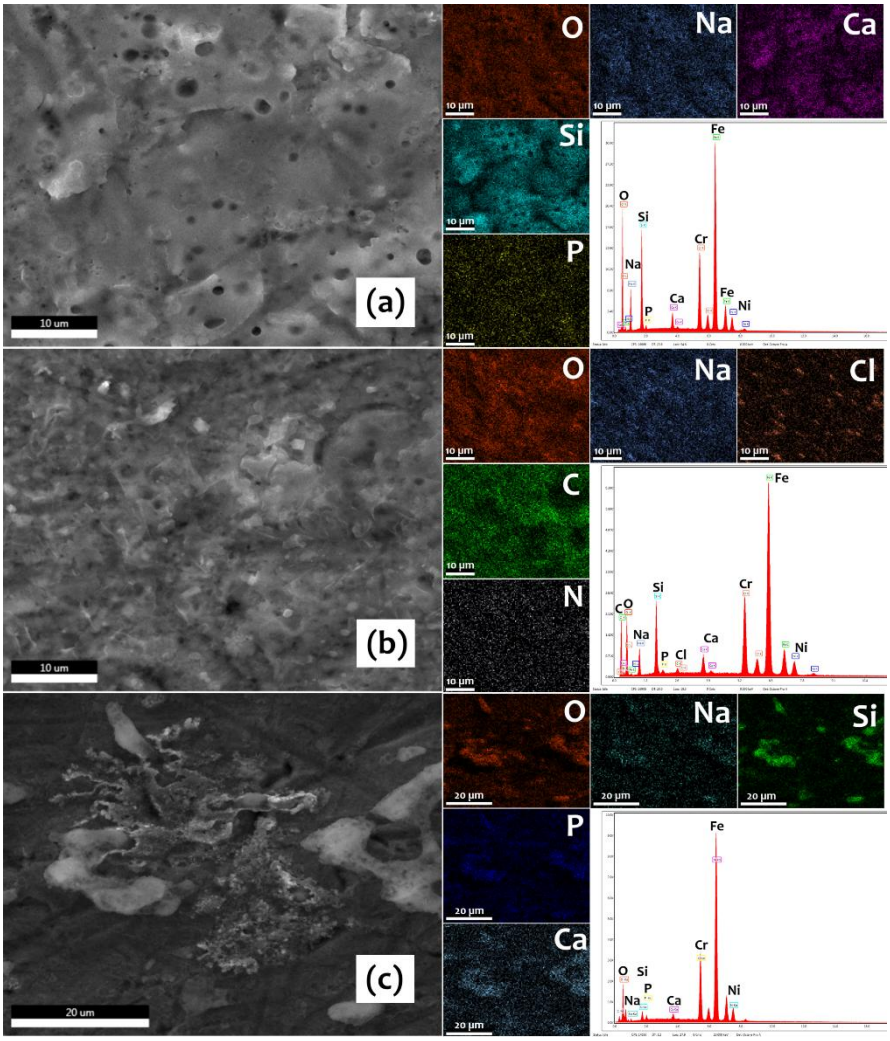

Fig. 7 a) EDS analysis of a specific area on the surface of the bioactive glass layer applied to the stainless steel substrate. b) EDS analysis of a specific area on the surface of substrates coated with Miramistin. c) EDS analysis of a specific area on the surface after 14 days of immersion in SBF.

Fig. 7a presents an SEM image with EDS analysis of an area coated with bioactive glass. In the image on the left, the rough texture of the surface and the presence of pores of varying sizes are observed. EDS analysis provides elemental mapping of the components of the bioactive glass, highlighting a relatively uniform element distribution. The presence of all elements characteristic of the composition of the bioactive glass confirms the formation of the desired layer. The EDS spectrum indicates the presence of peaks corresponding to the elements O, Na, Ca, Si and P from the bioactive glass, as well as peaks for Cr, Fe and Ni, originating from the stainless steel substrate. These observations suggest that the obtained coating has a uniform composition across the entire analyzed surface. Fig. 7b shows a SEM image with EDS analysis of an area initially covered with bioactive glass, followed by the application of Miramistin. In the image on the left, it can be observed that the presence of pores is no longer that obvious, probably due to their filling with Miramistin. Small cubic crystals can also be identified, which may correspond to NaCl crystals. This phenomenon may result from the interaction between bioactive glass and Miramistin, leading to the formation of sodium chloride. EDS analysis indicates a uniform distribution of Miramistin-specific elements (C and N). Small Cl clusters can confirm the composition of the cubic crystals. From the EDS spectrum, peaks corresponding to the elements in the composition of the bioactive glass, Miramistin and stainless steel supports are observed, suggesting that the Miramistin deposition is distributed over the entire analyzed surface. Fig. 7c shows a SEM image with EDS analysis of an area on the surface of the samples after 14 days of immersion in SBF. A relatively uniform distribution of all elements characteristic of hydroxyapatite is observed, and the composition of the agglomerates and the entire surface is similar, thus confirming the conclusions discussed in the SEM analysis section.

4. Conclusions

This study demonstrated the possibility of coating stainless steel supports with 45S5 bioactive glass using the spin-coating technique. The deposition of an additional layer of Miramistin improved the antimicrobial properties of the material. FTIR and SEM analyses confirmed the formation of uniform, slightly rough coatings, without macrocracks, with optimal adhesion to the stainless steel substrate. The distribution of bioactive glass and Miramistin on the surface was relatively homogeneous. Immersion in the SBF solution revealed the ability of the bioactive glass layer to induce the formation of hydroxyapatite, thus indicating high bioactivity. In addition, FTIR analysis confirmed the release of Miramistin into the SBF solution from the applied layer. These findings highlight the potential of this dual-layer approach in developing implantable materials with enhanced antimicrobial protection and bioactivity.

REFERENCES

[1] S. Hu, J. Chang, M. Liu, C. Ning, Study on antibacterial effect of 45S5 Bioglass, Journal of Materials Science: Materials in Medicine 20 (2009) 281-286.
[2] T. Waltimo, T.J. Brunner, M. Vollenweider, W.J. Stark, M. Zehnder, Antimicrobial Effect of Nanometric Bioactive Glass 45S5, Journal of Dental research 86(6) (2007) 754-757.
[3] C. Zhang, Y. Ru, J. You, R. Lin, S. Chen, Y. Qi, D. Li, C. Zhang, Z. Qiu, Antibacterial Properties of PCL@45s5 Composite Biomaterial Scaffolds Based on Additive Manufacturing, Polymers 16 (2024) 3379.
[4] E. Piatti, M. Miola, E. Verné, Tailoring of bioactive glass and glass-ceramics properties for in vitro and in vivo response optimization: a review, Biomater. Sci. 12 (2024) 4546-4589.
[5] Mîrț Andreea-Luiza, Denisa Ficai, Ovidiu-Cristian Oprea, G. Vasilievici, A. Ficai, Current and Future Perspectives of Bioactive Glasses as Injectable Material Nanomaterials 14(14) (2024) 1196.
[6] A.S. Pádua, S.R. Gavinho, T. Vieira, I. Hammami, J.C. Silva, J.P. Borges, M.P.F. Graça, In Vitro Characterization of Doped Bioglass 45S5/HAp Coatings Obtained by CoBlastTM Deposition, Coatings 13 (2023) 1775.
[7] M. Maximov, O.-C. Maximov, L. Craciun, D. Ficai, A. Ficai, E. Andronescu, Bioactive Glass—An Extensive Study of the Preparation and Coating Methods, Coatings 11(11) (2021) 1386.
[8] Z. Ling, X. Ge, C. Jin, Z. Song, H. Zhang, Y. Fu, K. Zheng, R. Xu, H. Jiang, Copper doped bioactive glass promotes matrix vesicles-mediated biomineralization via osteoblast mitophagy and mitochondrial dynamics during bone regeneration, Bioactive Materials 46 (2025) 195-212.
[9] A. Osmanov, Z. Farooq, M.D. Richardson, D.W. Denning, The antiseptic Miramistin: a review of its comparative in vitro and clinical activity, FEMS Microbiol Reviews 44(4) (2020) 399-417.
[10] T.V. Vasil'eva, A.S. Raskidaĭlo, A.A. Arutcheva, G.G. Okropiridze, A.A. Petrakov, Z.I. Urazgil'deev, T.M. Kovalenko, Antibacterial activity and clinical effectiveness of the new antiseptic miramistin, Antibiotics and chemoterapy 38(8-9) (1993) 61-63.
[11] A. Osmanov, A. Wise, D.W. Denning, In vitro and in vivo efficacy of miramistin against drug-resistant fungi Journal of medical microbiology 68(7) (2019) 1047-1052.
[12] Chernysheva M.G., Badun G.A., P. A.G, C.I. S., A.N. M., P.A. V., Preparation of Nanodiamond–Lysozyme–Miramistin Composite and Prospects of Its Application in Heart Valve Prosthetics, Colloid J 86 (2024) 120-129.
[13] L.D. Soule, N.P. Chomorro, K. Chuong, N. Mellott, N. Hammer, K.D. Hankenson, X. Chatzistavrou, Sol-Gel-Derived Bioactive and Antibacterial Multi-Component Thin Films by the Spin-Coating Technique ACS Biomater Sci Eng. 6(10) (2020) 5549-5562.
[14] T. Kokubo, H. Takadama, How useful is SBF in predicting in vivo bone bioactivity?, Biomaterials 27 (2006) 2907-2915.
[15] A. Motealleh, S. Eqtesadi, A. Civantos, A. Pajares, P. Miranda, Robocast 45S5 bioglass scaffolds: in vitro behavior, J. Mater. Sci. 52 (2017) 9179-9191.
[16] O.V. Dement'eva, V.M. Rudoy, One-pot synthesis and loading of mesoporous SiO2 nanocontainers using micellar drug as a template, RSC Advanced 6(42) (2016) 36207-36210.
[17] S.M. Shaban, I. Aiad, A.R. Ismail, Surface Parameters and Biological Activity of N-(3-(Dimethyl Benzyl Ammonio) Propyl) Alkanamide Chloride Cationic Surfactants, Journal of Surfactants and Detergents 19(3) (2016) 501-510.